A Novel Boron-rich Scandium Borocarbide; $Sc_{4.5-x}B_{57-y+z}C_{3.5-z}$ (x = 0.27, y = 1.1, z = 0.2)

Takaho Tanaka*, Akiji Yamamoto and Akira Sato

Advanced Materials Laboratory, National Institute for Materials Science

Namiki 1-1, Tsukuba, Ibaraki 305-0044, Japan

*To whom correspondence should be addressed.

E-mail: TANAKA.Takaho@nims.go.jp

Abstract

A novel ternary boron-rich scandium borocarbide $Sc_{4.5-x}B_{57-y+z}C_{3.5-z}$ (x = 0.27, y = 1.1, z = 0.2) was found. Single crystals were obtained by the floating zone method by adding a small amount of Si. Single-crystal structure analysis revealed that the compound has an orthorhombic structure with lattice constants of $a = 1.73040(6)$, $b = 1.60738(6)$ and $c = 1.44829(6)$ nm and space group *Pbam* (No.55). The crystal composition $ScB_{13.3}C_{0.78}Si_{0.008}$ calculated from the structure analysis agreed with the measured composition of $ScB_{12.9}C_{0.72}Si_{0.004}$. The orthorhombic crystal structure is a new structure type of boron-rich borides and there are six structurally independent B_{12} icosahedra I1 - I6, one B_8/B_9 polyhedron and nine bridging sites all which interconnect each other to form a three-dimensional boron framework. The main structural feature of the boron framework structure can be understood as a layer structure where two kinds of boron icosahedron network layer L1 and L2 stack each other along the *c*-axis. There are seven structurally independent Sc sites in the open spaces between the boron icosahedron network layers.

1. INTRODUCTION

During crystal growth and structure analysis work for a cubic scandium borocarbosilicide $Sc_{0.83-x}B_{10.0-y}C_{0.17+y}Si_{0.083-z}$ (1) whose composition obtained by structure analysis is $ScB_{12.0}C_{0.65}Si_{0.071}$, we could find two more new phases whose chemical compositions are very close to that of the cubic phase. One has an orthorhombic crystal structure with lattice constants of $a = 1.73040(6)$, $b = 1.60738(6)$ and $c = 1.44829(6)$ nm and space group *Pbam* (No.55) and its chemical composition measured by EPMA was $ScB_{12.9}C_{0.72}Si_{0.004}$. Another whose chemical composition was $ScB_{11.7}C_{0.6}Si_{0.04}$ has a hexagonal crystal structure and will be reported elsewhere (2).

We have reported subsolidus phase relations at 1700 °C in the ternary Sc-B-C system (3) where we have not detected the existence of both orthorhombic and hexagonal phases. Because of so small an Si content in the orthorhombic phase, we expected that it can exist without Si, which would request to add it to the previous Sc-B-C subsolidus phase relation. Several solid-state-reaction experiments soon proved that it can exist without Si as a ternary Sc-B-C system phase. In this paper, we describe phase and crystal structure analyses of the orthorhombic scandium borocarbide $Sc_{4.5-x}B_{57-y+z}C_{3.5-z}$ (x = 0.27, y = 1.1, z = 0.2).

2. EXPERIMENTAL

Raw powders of ScB_x were synthesized by a borothermal reduction method using a powder of Sc_2O_3 (3N, Crystal Systems Inc., Japan) and amorphous boron (2N, SB-Boron Inc., USA). The reaction was carried out in a boron nitride crucible using an RF heating furnace under vacuum for several hours at about 1700 °C, where a carbon-free composite susceptor was used instead of a graphite susceptor in order to avoid unexpected carbon contamination. After mixing suitable amount of B_4C powder (3N, Koujundo Kagaku Inc., Japan) to the obtained ScB_x powder, the mixed powder was pressed into a pellet by cold isostatic press process at 250 MPa and was sintered by the same way used for the ScB_x synthesis except for use of the graphite susceptor.

For the Sc-B-C ternary system, the floating zone crystal growth was actually impossible because the molten zone had a very strong tendency of swelling up to the feed rod. Thus, a small amount of Si was added to the raw powder in order to suppress the molten zone from swelling up. Further details of the floating zone crystal growth and chemical analysis are described elsewhere (1).

For EPMA measurement, ScB_{12} and $B_{4.5}C$ crystals were used as a standard for Sc, B and C analyses and an SiC crystal was used as an Si standard. The cubic-phase crystal of $ScB_{12}C_{0.7}Si_{0.1}$ whose composition was determined by wet chemical analysis was also used as an internal comparison.

Phase identification was carried out using a standard powder X-ray diffractometer (R-2000, Rigaku Co., Japan) with CuKα radiation. The single-crystal X-ray diffraction data were collected by two ways: (1) an imaging plate Weissenberg camera (Mac Science Co., Japan) with graphite-monochromated NbKα radiation and (2) an Enraf-Nonius CAD4 automatic four-circle

diffractometer with graphite-monochromated MoKα radiation. The crystal data and the four-circle intensity measurement data are given in Table 1. The intensity data were corrected for Lorenz and polarization effects. The absorption correction applied to the collected data was empirical based on Ψ-scans.

Table 1. Crystallographic and Data Collection Parameters

Chemical composition	$ScB_{12.8}C_{0.73}Si_{0.004}$ (obtained by EPMA measurement)
Crystal system	Orthorhombic
Space group	*Pbam* (No. 55)
Lattice constants (nm)	$a = 1.73040(6)$, $b = 1.60738(6)$, $c = 1.44829(6)$
Unit cell volume (nm^3)	4.0283(3)
Empirical formula	$Sc_{4.23}B_{56.4}C_{3.3}Si_{0.033}$ ($ScB_{13.3}C_{0.78}Si_{0.008}$)
	or $Sc_{4.5-x}B_{57-y+z}C_{3.5-z}$(x = 0.27, y = 1.1, z = 0.2)
Z	8
D_x (g/cm^3)	2.772
D_m (g/cm^3)	2.803
μ for MoKα (cm^{-1})	14
Crystal dimensions (mm)	0.18 (110) x 0.30 (110) x 0.25 (001)
$2\theta_{max}$	70°
Reflection measured	$-20 \leq h \leq 27$, $0 \leq k \leq 25$, $0 \leq l \leq 23$
Structure-refinement program	SHELXL97
R1	0.044 ($F_0 > 4s(F_0)$) for 5752, 0.102 (all F_0, for 9122 F_0)
wR2	0.117 (F^2)
Number of variables	322

3. RESULTS AND DISCUSSION

3.1. Phase analysis

In boron-rich part of the subsolidus Sc-B-C phase diagram (3) three ternary compounds of $ScB_{17}C_{0.25}$, $ScB_{15}C_{0.8}$ and $ScB_{15}C_{1.6}$ have been established. Floating zone crystal growth could be successfully applied to the $ScB_{15}C_{0.8}$ phase where a small amount of Si was necessary as mentioned above; however, crystal growth itself was not so easy (1). The single-crystal growth was carried out using a feed rod whose composition was $ScB_{15}C_{0.8}Si$. The molten zone was rather unstable. The zone-passed rod consisted of the central single-crystal region and the peripheral mixed-phase region which included additional B_4C. Single-crystal structure analysis and chemical analysis showed coincidentally that the obtained single-crystal part has a composition of about

3
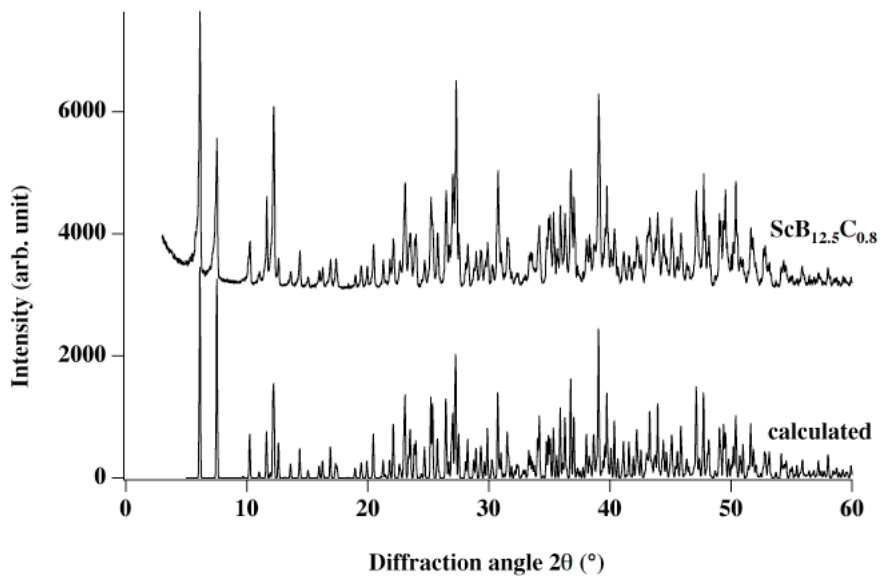
Fig. 1. The powder XRD pattern of $ScB_{12.5}C_{0.8}$ synthesized by solid-state reaction and the XRD pattern calculated based on the structure model.

I. $ScB_{15}C_{0.8}$

II. $ScB_{15}C_{1.6}$

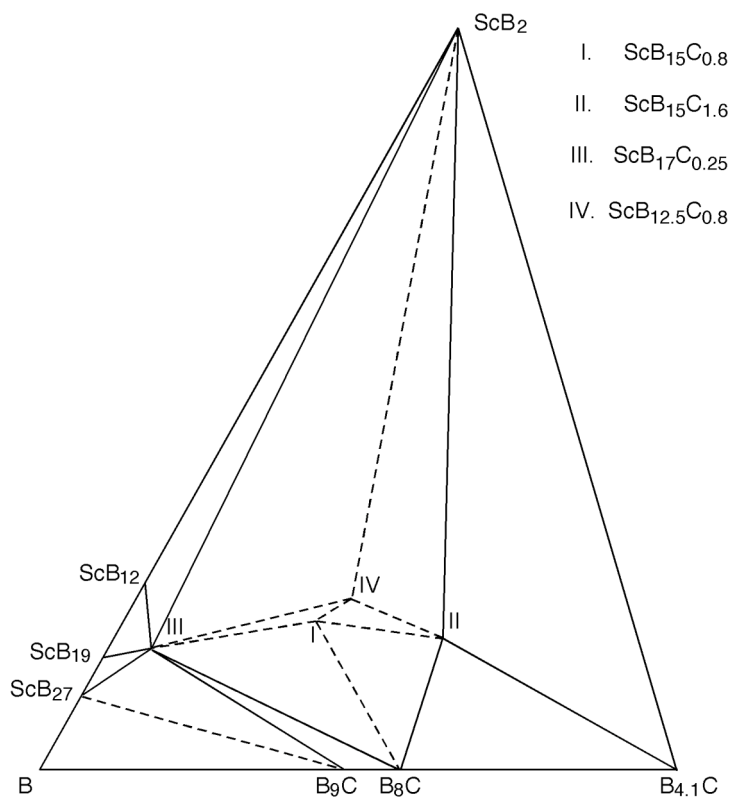III. $ScB_{17}C_{0.25}$

IV. $ScB_{12.5}C_{0.8}$

Fig. 2. The revised subsolidus phase diagram of the ternary Sc-B-C system at 1700°C.

$ScB_{12}C_{0.7}Si_{0.1}$. It was understood that the melt-growth method could increase site occupancy of Sc than the solid-state reaction method. The large difference of composition between the raw rod and the crystal caused quite unstable zone pass. Thus, for better crystal growth a raw powder of $ScB_{12}C_{0.7}$ was synthesized by solid-state reaction. The powder $ScB_{12}C_{0.7}$ should be a mixture of ScB_2, $ScB_{15}C_{0.8}$ and $ScB_{15}C_{1.6}$ according to the previous subsolidus phase diagram (3); however, the dominant peaks of the powder XRD pattern could be assigned to none of them and the $ScB_{15}C_{0.8}$ phase could be detected as a minor phase. Single phase was obtained around the composition of $ScB_{12.5}C_{0.8}$. Oxygen impurity of the samples was about 0.1 wt%. The single-phase powder pattern is shown in Fig. 1 from $2\theta = 5$ to $70°$. Above $70°$, XRD intensities become fairly weak and are not shown. Strong two peaks at $6.14°$ and $7.54°$ are characteristic in the powder pattern. Above $10°$, there are so many reflection peaks and the powder pattern is very complicated; however, it could be indexed as an orthorhombic structure with lattice constants of $a = 1.7296(2)$, $b = 1.6059(2)$ and $c = 1.4471(1)$ nm. In the figure, the experimental powder pattern is compared with that calculated from a structure model given later. Their coincidence is quite significant.

The orthorhombic crystal structure was realized later as a single-crystal form by addition of a very small amount of Si. The result requests us to add the new orthorhombic phase to the previous subsolidus phase diagram. The corrected one is shown in Fig. 2 where the orthorhombic phase is shown as phase IV with the representative composition of $ScB_{12.5}C_{0.8}$. On the other hand, the hexagonal phase $ScB_{11.7}C_{0.6}Si_{0.04}$ mentioned in the previous section could not be synthesized as a ternary Sc-B-C phase compound up to now. Structure analysis showed that its Si site is a key position of the hexagonal structure. Probably, the phase can exist only as a quaternary Sc-B-C-Si compound so that it should not be included in the ternary phase diagram.

3.2. Structure analysis

At first, a single crystal was accidentally grown at the initial stage of the crystal growth of the cubic $Sc_{0.83-x}B_{10.0-y}C_{0.17+y}Si_{0.083-z}$ (1). Several crystal-growth experiments followed and the size of the obtained crystals achieved a macroscopic one of more than 8 mm in diameter and 5 mm long. However, it was difficult to grow the orthorhombic-phase crystal through whole crystal rods. The orthorhombic-phase crystal appeared at the initial stage of those crystal-growth experiments and at the latter part the cubic-phase crystal grew. Appropriate crystal-growth conditions such as the feed rod composition and the molten zone composition were not established yet.

A single-crystal specimen for single-crystal XRD data collection could be obtained by cracking a part of the grown crystal. The density of the crystal was measured by a standard buoyancy method using hexachloro-1, 3-butadiene as a buoyancy medium and an Si single crystal as the density standard: 2.330 g/cm³. The measured density was 2.803 g/cm³. The part remained was sent to EPMA measurement. The obtained Sc, B, C and Si contents were 23.3 ± 0.6, 72.0 ± 0.6, 4.5 ± 0.2 and 0.05 ± 0.004 wt%, respectively and the sum of each mean value is 99.85 wt%. Since each value was determined independently, the fact that the total sum became almost 100 wt% proved the high reliability of the measured values. The normalized chemical

composition is $ScB_{12.9}C_{0.72}Si_{0.004}$. Oxygen impurity in the crystal was undetectable by the EPMA measurement because most of the oxygen impurity in the feed rod evaporated out during the melt crystal-growth process.

The crystal quality was checked by Weissenberg camera prior to the single-crystal XRD data collection. Further, we collected the single crystal XRD data by the imaging plate Weissenberg camera as well as by the four-circle diffractometer as mentioned before, we could reject a possibility of twinning in the specimen. The coincidence between the experimental powder XRD pattern and the calculated one shown in Fig. 1 also denies the possibility of twinning. Although the structure refinements using both data sets gave almost same results, the four-circle diffractometer data set gave slightly better *R1* and *R2* values; thus, this will be used for discussion hereafter.

An initial solution was obtained by SIR92 (4) according to the space group *Pbam* (No. 55) and the program SHELXL-97 (5) was used for refinement. The direct method gave 78 atomic positions in which seven Sc, six C, 65 B sites and no Si site were assigned. At this stage, *R1* value was 5.3% with 314 parameters for 5368 independent reflections ($F_o > 4\sigma(F_o)$). Visualization of the crystal structure using the graphic program CrystalMaker (6) immediately showed a three-dimensional boron framework composed of interconnected B_{12} icosahedra, another boron polyhedra and bridging boron or carbon sites. Careful examination of both bond distances and temperature factors suggested us that some C sites should be turned to B sites. However, Si site was not found. On refinement, partial occupancy was applied to all Sc sites and three B sites, the latter have unusually short bonding distances. Moreover, one B site was reassigned to a site occupied either of B or C, so-called a mixed-occupancy site. Thus, seven partially occupied Sc, four C, 66 B sites with three partially occupied sites and one B/C mixed-occupancy site are counted in the orthorhombic $Sc_{4.5-x}B_{57-y+z}C_{3.5-z}$ crystal structure, where the numbers in the suffixes are the total number of the sites divided by maximum multiplicity of 8, x and y describe the partial occupancy of sites and z describes the B/C mixed occupancy. The values of x, y and z for the present crystal are 0.27, 1.1 and 0.2, respectively.

The crystal used for XRD data collection has included a small amount of Si. There remained a question, at which site does Si reside? Actually, one of B partial occupancy sites can only be a candidate. The nearest-neighbor bonding distances of the site are 1.838, 1.863, 1.964 and 2.022 Å. When both partial occupancy and mixed occupancy are simultaneously applied to the site, SHELXL could not converge. Thus, B and Si occupancies to the site were fixed and their suitable combination was manually searched; resultantly, the occupancy B + Si = 30 % (B/Si=0.9/0.1) was obtained to the B/Si71 site as listed in Table 2.

The final refinement of 322 parameters for 5752 independent reflections ($F_o > 4\sigma(F_o)$) resulted in the *R1* value of 4.4 % and 10.2 % for all 9122 independent reflections. The normalized composition $ScB_{13.3}C_{0.78}Si_{0.008}$ obtained by the structure refinement agrees rather well with that of $ScB_{12.9}C_{0.72}Si_{0.004}$ obtained by EPMA measurement. The final atomic coordinates, occupancy factors and temperature factors are listed in Table 2.

Table 2.　Final atomic coordinates, occupancy factors and temperature factors.

Atom	Site	x	y	z	Occupancy	$U(Å^2x10^3)$
B1	8i	0.3347(1)	0.2050(2)	0.6241(2)	1	5.8(4)
B2	8i	0.1410(2)	-0.1034(2)	0.2728(2)	1	6.6(4)
B3	8i	0.2612(1)	0.2836(2)	0.6215(2)	1	5.8(4)
B4	8i	0.4280(1)	0.2589(2)	0.6235(2)	1	6.0(4)
B5	8i	0.3484(2)	0.2963(2)	0.5582(2)	1	5.3(4)
B6	8i	0.2823(1)	0.2312(2)	0.7301(2)	1	5.4(4)
B7	8i	0.3070(1)	0.3795(2)	0.6211(2)	1	5.1(4)
B8	8i	0.4055(1)	0.3652(2)	0.6226(2)	1	5.3(4)
B9	8i	0.3898(1)	0.2167(2)	0.7324(2)	1	5.8(4)
B10	8i	0.3476(2)	0.3034(2)	0.7929(2)	1	6.4(4)
B11	8i	0.2682(1)	0.3424(2)	0.7236(2)	1	5.1(4)
B12	8i	0.4371(2)	0.3209(2)	0.7295(2)	1	5.9(4)
B13	8i	0.4587(2)	-0.0243(2)	0.8542(2)	1	7.4(4)
B14	8i	0.3552(1)	-0.0209(2)	0.7027(2)	1	5.8(4)
B15	8i	0.3940(1)	0.0421(2)	0.7953(2)	1	5.4(4)
B16	8i	0.3019(2)	-0.0052(2)	0.8126(2)	1	6.5(4)
B17	8i	0.6125(2)	0.1769(2)	0.8143(2)	1	6.6(4)
B18	8i	0.5250(2)	0.1195(2)	0.7960(2)	1	5.9(4)
B19	8i	0.0752(2)	0.3872(2)	0.0943(2)	1	6.2(4)
B20	8i	0.6791(2)	0.1048(2)	0.8810(2)	1	6.3(4)
B21	8i	0.4539(2)	-0.0273(2)	0.7328(2)	1	5.7(4)
B22	8i	0.5951(2)	0.1197(2)	0.7028(2)	1	6.4(4)
B23	8i	0.3716(2)	-0.0065(2)	0.9054(2)	1	6.7(4)
B24	8i	0.1886(2)	0.3891(2)	0.2408(2)	1	6.1(4)
B25	4h	0.5570(2)	0.3161(2)	0.5000(0)	1	4.8(6)
B26	8i	0.5896(2)	0.1702(2)	0.6004(2)	1	6.1(4)
B27	4h	0.4658(2)	-0.1389(2)	0.5000(0)	1	5.9(6)
B28	8i	0.6782(1)	0.2169(2)	0.5618(2)	1	5.3(4)
B29	4h	0.3651(2)	-0.1350(2)	0.5000(0)	1	3.4(6)
B30	8i	0.5115(1)	0.2348(2)	0.5630(2)	1	5.4(4)
C31	4h	0.6546(2)	0.3025(2)	0.5000(0)	1	7.3(5)
B32	8i	0.6020(2)	0.2784(2)	0.6021(2)	1	5.7(4)
C33	4h	0.1831(2)	0.0261(2)	0.5000(0)	1	6.2(5)
C34	4h	0.3222(2)	-0.0486(2)	0.5000(0)	1	8.9(6)

B35	8i	0.2270(2)	0.0603(2)	0.6016(2)	1	6.3(4)
B36	8i	0.7354(1)	0.5437(2)	0.4379(2)	1	6.0(4)
B37	4h	0.7189(2)	0.3766(2)	0.5000(0)	1	6.4(6)
B38	4h	0.3734(2)	0.0459(2)	0.5000(0)	1	6.8(6)
B39	8i	0.3187(1)	0.0127(2)	0.6004(2)	1	5.6(4)
B40	8i	0.3098(2)	0.1178(2)	0.5629(2)	1	6.2(4)
B41	8i	0.4507(1)	0.4330(2)	0.5607(2)	1	5.2(4)
B42	8i	0.0390(2)	0.0341(2)	0.6004(2)	1	6.1(4)
C43	4h	0.5297(2)	0.4086(2)	0.5000(0)	1	7.7(6)
B44	4h	0.0943(2)	0.0123(2)	0.5000(0)	1	5.9(6)
B45	8i	0.2050(2)	0.1636(2)	0.7716(2)	1	6.0(4)
B46	8i	0.0681(2)	0.1263(2)	0.1059(2)	1	8.9(5)
B47	8i	0.6154(1)	0.3328(2)	0.7019(2)	1	5.3(4)
B48	8i	0.0749(2)	0.0661(2)	0.7017(2)	1	6.7(4)
B49	8i	0.1163(2)	0.2096(2)	0.8164(2)	1	6.3(4)
B50	8i	0.0317(2)	0.1444(2)	0.7735(2)	1	6.1(4)
B51	8i	0.0415(2)	0.0348(2)	0.1842(2)	1	7.5(4)
B52	8i	0.1772(1)	0.0777(2)	0.7000(2)	1	5.7(4)
B53	8i	0.1314(2)	-0.0047(2)	0.2313(2)	1	9.2(4)
B54	8i	0.1279(2)	0.0314(2)	0.1094(2)	1	18.9(6)
B55	8i	0.2129(2)	0.0524(2)	0.1870(2)	1	7.7(4)
B56	8i	0.1744(2)	0.1361(2)	0.1069(2)	1	9.2(5)
B57	8i	0.7574(2)	0.1419(2)	0.9408(2)	1	9.6(5)
B58	4g	0.8776(2)	0.2582(3)	0.0000(0)	1	9.5(6)
B59	8i	0.8460(2)	0.1852(2)	0.9102(2)	1	7.4(5)
B60	4g	0.2774(2)	0.2621(3)	0.0000(0)	1	10.1(7)
B61	4g	0.4196(3)	0.3404(3)	0.0000(0)	1	17.6(8)
B62	4g	0.1589(4)	0.8983(4)	0.0000(0)	0.58	6.0(16)
C/B63	8i	0.4300(1)	0.1383(1)	0.7908(2)	C/B=0.80/0.20	6.2(4)
B64	4g	0.1305(4)	-0.0080(4)	0.0000(0)	0.78	14.9(15)
C65	4h	0.5219(2)	-0.0431(2)	0.5000(0)	1	12.6(6)
B66	4g	0.9242(3)	0.3500(3)	0.0000(0)	1	11.9(7)
B67	4g	0.2231(2)	0.1635(2)	0.0000(0)	1	8.6(6)
B68	4g	0.0246(2)	0.3536(2)	0.0000(0)	1	6.8(6)
B69	4g	0.5216(2)	0.3482(3)	0.0000(0)	1	8.3(6)
B70	4g	0.8751(2)	0.4428(3)	0.0000(0)	1	10.3(7)

B/Si71	8i	0.1440(4)	0.9256(4)	0.0604(4)	B+Si=0.30 (B/Si=0.9/0.1)	6.4(10)
Sc1	8i	0.47761(2)	0.24988(3)	0.88052(3)	0.97	6.0(1)[a]
Sc2	2a	0.50000(0)	0.50000(0)	0.00000(0)	0.96	14.9(3)[a]
Sc3	8i	0.44587(3)	0.10615(3)	0.63668(3)	0.97	6.2(1)[a]
Sc4	8i	0.31793(3)	0.15473(3)	0.87857(3)	0.97	7.1(1)[a]
Sc5	4g	0.13723(4)	0.27037(4)	0.00000(0)	0.96	8.8(2)[a]
Sc6	4g	0.24837(5)	0.00566(5)	0.00000(0)	0.9	9.3(2)[a]
Sc7	2c	0.50000(0)	0.00000(0)	0.00000(0)	0.61	8.3(4)[a]

	U_{11}	U_{22}	U_{33}	U_{23}	U_{13}	U_{12}
Sc1	5.5(2)	7.6(2)	4.9(2)	-0.8(2)	0.2(1)	0.4(2)
Sc2	14.2(5)	15.2(5)	15.2(5)	0	0	4.9(4)
Sc3	7.4(2)	5.6(2)	5.5(2)	-0.3(1)	0.3(2)	1.2(1)
Sc4	4.4(2)	11.5(2)	5.4(2)	0.1(2)	0.7(1)	-0.3(2)
Sc5	5.8(3)	11.2(3)	9.5(3)	0	0	3.0(2)
Sc6	10.3(3)	8.3(3)	9.4(3)	0	0	-2.6(3)
Sc7	11.3(7)	10.7(7)	2.9(6)	0	0	-4.6(5)

[a]For Sc sites anisotropic thermal factors are applied and U_{eq} (one third of the trace of the orthogonarized U_{ij} tensor) is denoted in these columns.

Usually, the measured crystal density is lower than the calculated density because of the pore-like crystal imperfections. However, for the present crystal the measured density of 2.803 g/cm^3 is higher than the calculated one, 2.772 g/cm^3. Probably, the Sc site occupancies are underestimated due to the use of neutral Sc atom for the refinement. Rare earth elements are expected to be ionized in boron-rich borides. On the structure refinement of YB$_{62}$ and YB$_{56}$, occupancy of the Y site increased with an increase in charge number of Y and the atomic ratio approached YB$_{62}$ or YB$_{56}$ determined by chemical analysis (7). However, such treatment is rather time consuming and should not be the subject of the present paper. Instead, a simple assumption was tried; if the total Sc site occupancy in the empirical formula was increased from 4.23 to 4.39 in order to adjust the [B]/[Sc] ratio to that obtained by EPMA measurement, the calculated density would become 2.796 g/cm^3 which almost coincides to the measured density.

In the crystal structure, there are six structurally independent icosahedra I1, I2, I3, I4, I5 and I6 which are formed by B1-B12, B13-B24, B25-B32, C33-B40, B41-B44 and B45-B56, respectively as grouped in Table 2. B57-B62 forms a B$_8$ polyhedron. The B$_8$ polyhedron is connected to two icosahedra I6 through the bridging B64 atom as shown in Fig. 3(a). However, both B62 and B64 sites are only partially occupied with the occupancies of 58 % and 78 %, respectively. Although their calculated occupancies are somewhat different, probably their existence/absence is coupled. When they are absent, another configuration shown in Fig. 3(b) can

be realized, where a B_9 polyhedron is formed. Two B/Si71 atoms replace the B62 atom and the B_9 polyhedron is directly connected to the icosahedra I6. The occupancy 30 % of the B/Si71 is a reasonable value as compared with the B62 and B64 site occupancies. Si seldomly occupies the B/Si71 site, but the Si occupation is not indispensable because this phase can exist without Si as mentioned before. Boron atoms B54 and B61 have fairly large temperature factors although their site occupancies are 100 %. Probably, these sites are slightly different between the two configurations and the differences are not so large as those to be expressed as a split site but appeared as seemingly large temperature factors.
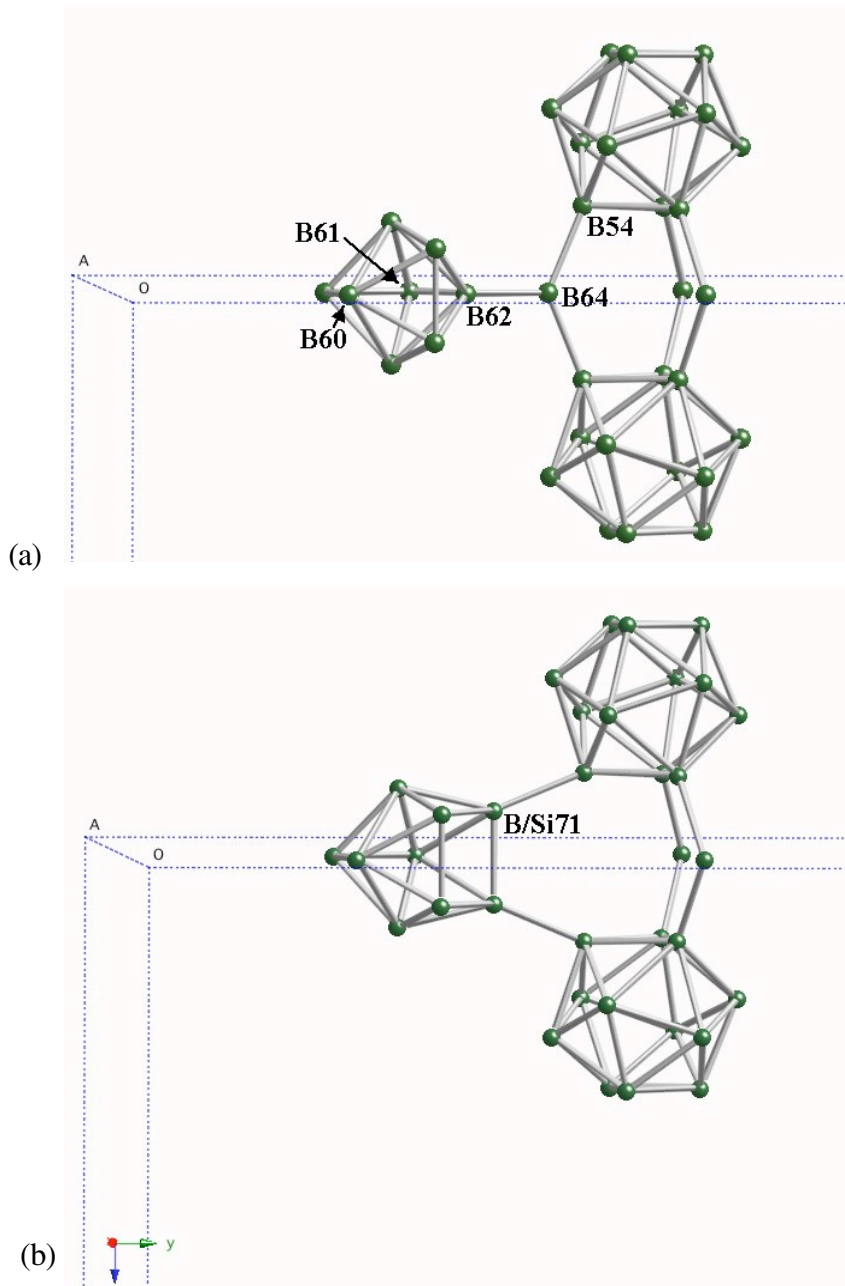
Fig. 3. The B_8/B_9 polyhedron connection to the icosahedra I2, (a) the case of the B_8 polyhedron and (b) the case of the B_9 polyhedron.

The intraicosahedral bond distances of each icosahedron range from 1.721 Å to 1.876 Å for I1, 1.703 Å to 1.940 Å for I2, 1.691 Å to 1.834 Å for I3, 1.682 Å to 1.838 Å for I4, 1.671 Å to 1.774 Å for I5 and 1.770 Å to 1.938 Å for I6 and their average values are 1.797, 1.811, 1.773, 1.775, 1.723 and 1.847 Å, respectively. The icosahedra I3, I4 and I5 are smaller than I1, I2 and I6 because they include carbon atoms. The intrapolyhedron bond distances of the B_8 polyhedron range from 1.717 Å to 1.958 Å and for the case of the B_9 polyhedron the longest bond distance increases up to 2.022 Å. Such a long bond distance allows Si accommodation in the B_9 polyhedron as discussed before. The intericosahedral B-B bond distances and the B-B distances for linkage between the icosahedron and the B_8/B_9 polyhedron range from 1.613 Å to 1.842 Å and the intericosahedral B-C distances range from 1.553 Å to 1.573 Å. The bond lengths for linkage between bridge sites and polyhedron units or other bridge sites range from 1.577 Å to 1.863 Å. The shortest one corresponds to the C65-C65 distance and the longest one corresponds to the B/Si71-B54 distance, respectively. The variations of any kinds of bond distances mentioned above are fairly wider than those of the previously reported cubic $Sc_{0.83-x}B_{10.0-y}C_{0.17+y}Si_{0.083-z}$ (1). Its intra- and intericosahedral bond distances range only from 1.728(7) to 1.890(9) and from 1.647(7) to 1.778(7) Å, respectively, except for special B,C(6)-B,C(6) bonds which are 1.716 Å and 1.615 Å for the intra- and intericosahedral bonds, respectively. Probably, the wide variety of the bond length of the present orthorhombic phase is due to the more complicated crystal structure than the previous cubic phase. In fact, the number of independent atoms 78 of the orthorhombic phase is just three times of that (26) of the cubic phase although the number of total atoms 520 in the unit cell is about half of that (1064) of the cubic phase. Thus, in the cubic phase carbon accommodation can be seen only one of three icosahedra and the C(1) bridg site. On the other hand, in the present orthorhombic phase carbon accommodates three of the six icosahedra and two bridge sites.

3.3. Description of the structure

The crystal structure of $Sc_{4.5-x}B_{57-y+z}C_{3.5-z}$ is characterized by a boron framework structure as usual boron-rich borides. There are two ways of understanding the boron framework structure. In one way, larger structure units formed by several icosahedra have been introduced. In the crystal structure description of YB_{66} (8), a super icosahedron of $B_{12}(B_{12})_{12}$ which is made up by 13 icosahedra was introduced and the supericosahedron forms a face-centered cubic lattice locating at the face-centered cubic lattice points in one orientation and at the centers of the cell and the cell edges rotated by 90°. The crystal structure of the previous cubic phase was also described by introducing two supertetrahedra and one superoctahedron (1). They are formed basically by four and six icosahedra, respectively. In another way, network linkage between icosahedra and polyhedra have been considered. A typical example is given by Higashi (9) who demonstrated beautiful network arrangements between icosahedra and between B_{20} units in the boron framework structure of α-AlB_{12} and γ-AlB_{12}.

For the present $Sc_{4.5-x}B_{57-y+z}C_{3.5-z}$ case, we could find a supericosahedron $B_{12}(B_{12})_{12}$ at the body center of the unit cell, however, there is no more super structure unit. Thus, it is difficult to

describe the whole boron framework structure by several super structure units. It is easier to understand the boron framework structure of $Sc_{4.5-x}B_{57-y+z}C_{3.5-z}$ as a layer structure where two kinds of boron icosahedron network layer stack each other along the *c*-axis. As shown in Fig. 4, one network layer L1 consists of three icosahedra I3, I4, I5 and the bridging carbon C65. The height of the layer L1 is $z = 0.5$. Another network layer L2 consists of I2 and I6 as shown in Fig. 5. The height of the layer L2 is $z = 0.196$ and 0.804. Thus, two L2 layers in the unit cell sandwich the layer L1. Large open spaces of both layers form channels along the *c*-axis. Actually, some structure units accommodate in the channels as will be mentioned later. By comparing two layers we can understand that the icosahedron I2 of the layer L2 locates above and below the hexagonal ring formed by I3, I4 and C65 "dimer" of the layer L1. The icosahedron I6 locates also above and bellow the hexagonal ring formed by the icosahedra I3, I4 and I5.
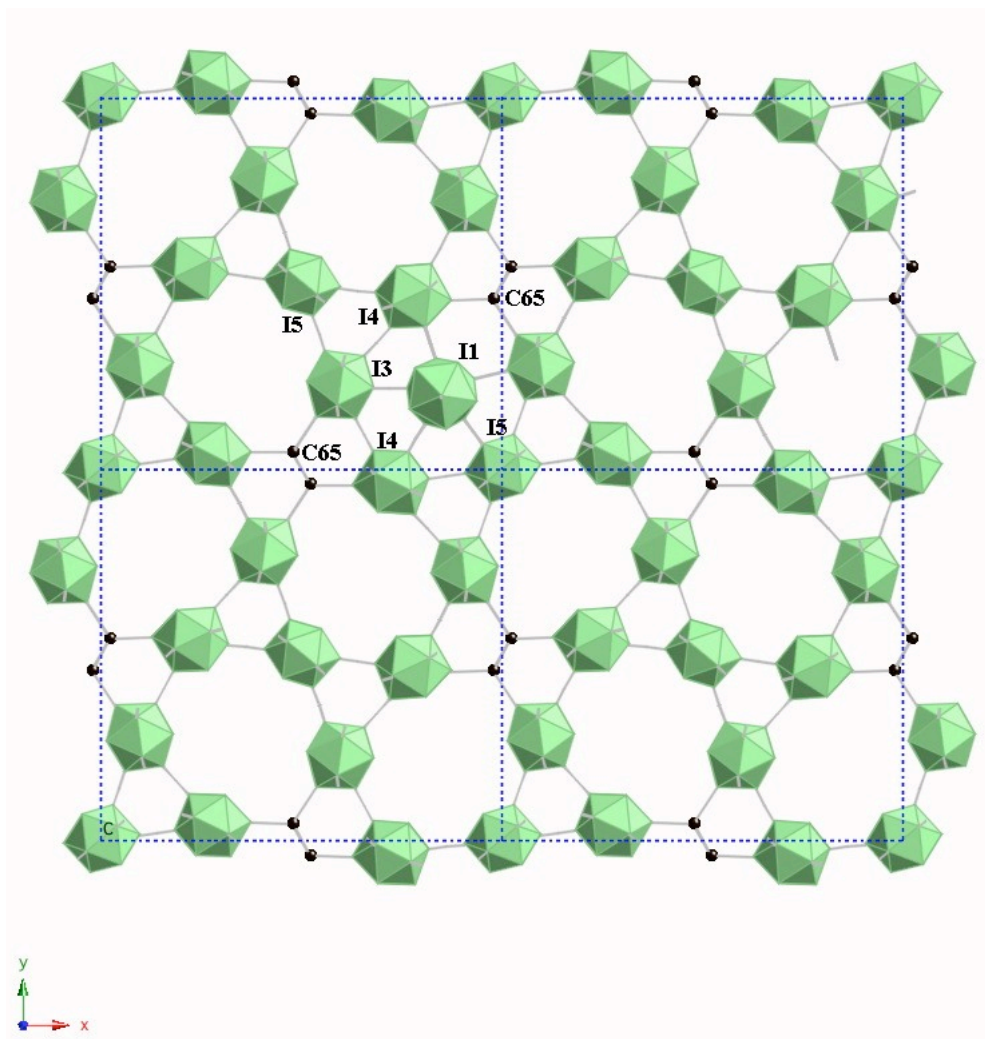

Fig. 4. The boron network layer L1 consists of the icosahedra I3, I4 and I5 and the C65 "dimer". Four unit cells are shown as a projection onto the (001) plane. An example of the connection of the icosahedron I1 to the layer L1 is also indicated. The icosahedron I1 which is sandwiched by the layers L1 and L2 situates in the large openings of the layers L1 and L2. The height of I1 from L1 is $z = \pm0.147$.
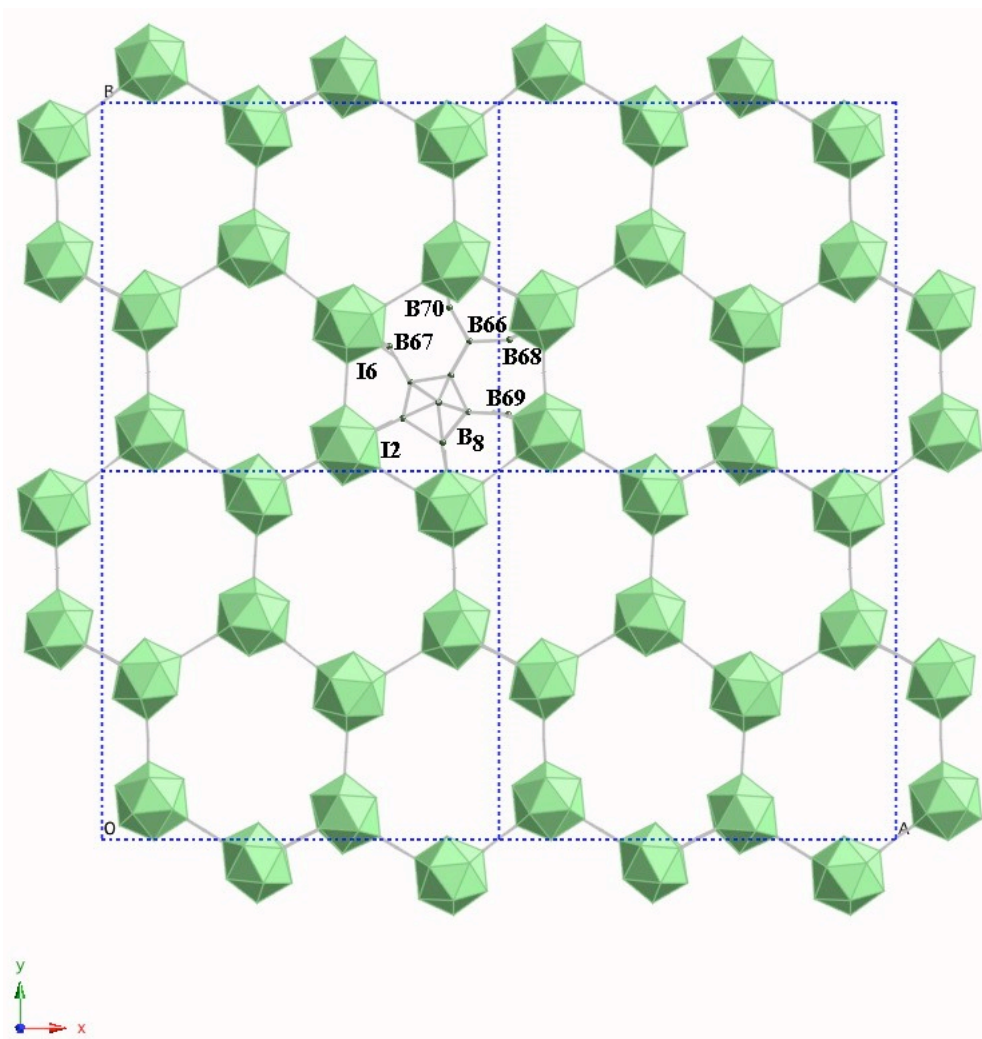
Fig. 5. The boron network layer L2 consists of the icosahedra I2 and I6. Four unit cells are shown as a projection onto the (001) plane. An example of the connection of the B_8 polyhedron to the layer L2 through the bridging atoms of B66 to B70 is also indicated. L2 sandwiches the B_8 polyhedron and the bridging atoms of B66 to B70.

The icosahedron I1 is one of the structure units accommodating in the channels formed by the layers L1 and L2. The height of the icosahedron I1 is z = 0.324 and 0.676. Thus, it locates middle of the layers L1 and L2 playing an important role of bridging both layers in addition to their direct bonding. An example of the icosahedron I1 arrangement on the layer L1 is indicated in Fig. 4.

The neighboring L2 layers, for example z = ±0.196, are separated about 5.7 Å. The distance is too large to directly bond each other. Thus, the B_8/B_9 polyhedra and several bridge site atoms contribute to bridge the neighboring L2 layers accommodating in the channels. An example of the B_8 polyhedron arrangement on the layer L2 is indicated in Fig. 5.

All Sc atoms reside open spaces between layers. Both Sc1 and Sc4 atoms locate at z = 0 between the L2 layers and are surrounded similarly by the icosahedra I1, I2, I6 and the B_8/B_9 polyhedron as shown in Fig. 6(a) and (b), respectively, where the B_8 polyhedron is depicted.
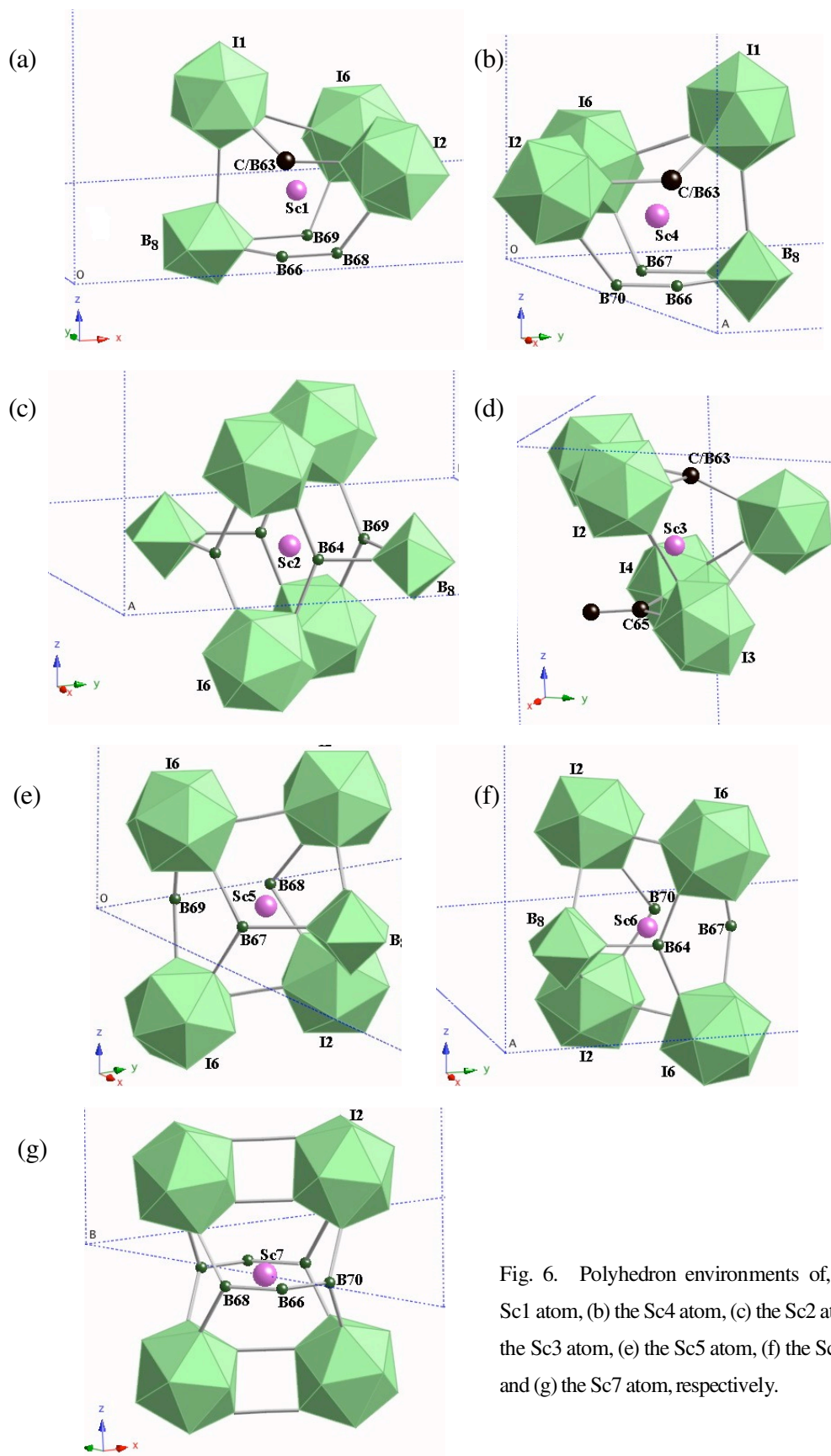
Fig. 6. Polyhedron environments of, (a) the Sc1 atom, (b) the Sc4 atom, (c) the Sc2 atom, (d) the Sc3 atom, (e) the Sc5 atom, (f) the Sc6 atom and (g) the Sc7 atom, respectively.

14

Hereafter, the B_8 polyhedron will be depicted as a representative of the B_8/B_9 polyhedron. The difference between them is coordinating bridge site atoms of B66 and B68 for the Sc1 atom and of B70 and B67 for the Sc4 atom, respectively. The nearest-neighbor distances of the Sc1 atom are 2.362 Å (C/B63), 2.451 Å (B58) and 2.464 Å (B69). The nearest-neighbor distances of the Sc4 atom are 2.334 Å (C/B63), 2.409 Å (B67) and 2.473 Å (B58).

The Sc2 atom locates at the corners of the unit cell and the face center of c-plane being coordinated by four icosahedra I6, two bridge site atoms B64 and two bridge site atoms B69 as shown in Fig. 6(c). Two B_8 polyhedra are added for easier understanding. The shortest and the second shortest distances are 2.262 Å (B64) and 2.468 Å (B69). The icosahedra I6 is rather far from the Sc2 atom and the shortest distance between them is 2.768 Å (B54). The Sc3 atom which lies between the layer L1 and the layer L2 is coordinated by the icosahedra I1, I2, I3 and I4 and the bridge site atoms of C/B63 and one of the C65 dimers as shown in Fig. 6(d). The C65 atom and the C/B63 atom are closest (2.299 Å) and second closest (2.309 Å) to the Sc3 atom, respectively. The icosahedron I1 is the closest (B9, 2.454 Å) in five coordinating icosahedra.

Both Sc5 and Sc6 atoms are also similarly coordinated by two icosahedra I2, two icosahedra I6 and one B_8 polyhedron as shown in Fig. 6(e) and 6(f), respectively. Their difference is surrounding bridge site atoms. The Sc5 atom is coordinated by the B67, B68 and B69 atoms and the Sc6 atom is coordinated by the B64, B70 and B67 atoms, respectively. The nearest-neighbor distances of the Sc5 atom are 2.271 Å (B67), 2.364 Å (B68) and 2.429 Å (B60) and those of the Sc6 atom are 2.051 Å (B64), 2.318 Å (B62) and 2.344 Å (B70), respectively. The space for the Sc6 atom is narrower than that for the Sc5 atom.

The environment of the Sc7 atom is rather symmetric because it locates at the special position of (0.5, 0, 0) as shown in Fig.5(g) where four icosahedra I2 and the bridge site atoms of B66, B68 and B70 are arranged. The figure also shows that the icosahedra I2 have an unusual double bonding which can be seen very seldom as the bonding between icosahedra (10, 11). The nearest-neighbor distances are 2.263 Å (B13), 2.349 Å (B70) and 2.391 Å (B68). Only the Sc7 site has a rather low site occupancy of 61% as compared with others all whose occupancies are 90% or more.

4. CONCLUSIONS

A novel compound $Sc_{4.5-x}B_{57-y+z}C_{3.5-z}$ is established as a newly found ternary Sc-B-C phase. The compound with the representative composition of $ScB_{12.5}C_{0.8}$ was synthesized by solid-state-reaction route and its single crystals were obtained by the floating zone method by adding a small amount of Si. Single-crystal structure analysis revealed that the compound $Sc_{4.5-x}B_{57-y+z}C_{3.5-z}$ has an orthorhombic structure with lattice constants of a = 1.73040(6), b = 1.60738(6) and c = 1.44829(6) nm and space group $Pbam$ (No.55). There are 78 structurally independent atoms in the unit cell, which are seven partially occupied Sc, four C, 66 B sites with three partially occupied sites, one B/C mixed-occupancy site. Six structurally independent icosahedra and one B_8/B_9 polyhedron are formed by most of these boron and carbon atoms. In

the crystal structure, these icosahedra form two kinds of network layers. The layers form a rigid boron framework stacking each other along the c-axis. Sc atoms occupy the open spaces between these boron icosahedron network layers.

This work forms a part of searching new rare earth boron-rich borides in order to find a replaceable material to YB_{66}. YB_{66} single crystal is useful as a soft X-ray monochromater for dispersing synchrotron radiation from 1 to 2 keV energy region (12, 13). Although YB_{66} satisfies almost material requirements for soft X-ray monochromater use, one exception is its amorphous-material-like low thermal conductivity. It makes difficult to use the YB_{66} monochromater extensively on brighter insertion device beam lines. In order to examine the applicability of the present $Sc_{4.5-x}B_{57-y+z}C_{3.5-z}$ phase, we need to grow its large and high-quality single crystals. However, floating zone crystal growth is not so successful up to now. After several millimeters zone pass, the orthorhombic phase stopped growing. Sc-B-C-Si quaternary phase relation must be investigated more in detail. Meanwhile, the present orthorhombic phase is Sc-B-C ternary phase, one may think that the crystal growth without Si should be tried. Actually, without Si the molten zone consisting of boron-rich melt including carbon always swells up to the feed rod and the zone pass was impossible. The Si addition prevents such swelling-up behavior of the melt.

ACKNOWLEDGMENTS

REFERENCES

1. T. Tanaka and A. Sato, *J. Solid State Chem.* **165**, 148 (2002).

2. T. Tanaka and A. Sato, *J. Solid State Chem.* to be submitted.

3. Y. Shi, A. Leithe-Jasper and T. Tanaka, *J. Solid State Chem.* **148**, 250 (1999).

4. A. Altomare, G. Cascarano, C. Giacovazzo, A. Guagliardi, M. Burla, G. Polidori and M. Camalli, *J. Appl. Cryst.* **27**, 435 (1994).

5. G. M. Sheldrick, SHELX97: a program for the solution and refinement of crystal structures, Universität Göttingen, Göttingen, Germany, 1997.

6. D. Palmer, *CrystalMaker* vers. 4.1.4, CrystalMaker Software, Bicester, Oxfordshire, OX6 7BS, UK.

7. I. Higashi, K. Kobayashi, T. Tanaka and Y. Ishizawa, *J. Solid State Chem.* **133,** 16 (1997)

8. S. M. Richards and J. S. Kasper, *Acta Crystallogr. Sect. B* **25**, 237 (1969).

9. I. Higashi, *J. Solid State Chem.* **154,** 168 (2000).

10. I. Higashi, T. Tanaka, K. Kobayashi, Y. Ishizawa and M. Takami, *J. Solid State Chem.* **133,** 11 (1997).

11. A. Leithe-Jasper, L. Bourgeois, Y. Michiue, Y. Shi and T. Tanaka, *J. Solid State Chem.* **154,** 130 (2000).

12. T. Tanaka, Z. U. Rek, Joe Wong and M. Rowen, *J. Cryst. Growth* **192**, 141 (1998).

13. Joe Wong, T. Tanaka, M. Rowen, F. Schäfers, B. R. Müller and Z. U. Rek, *J. Synchrotron Rad*. **6**, 1086 (1999).